Two-dimensional calculation of eddy currents on external conducting walls induced by low-*n* external modes

D.-Y. Lee[a)]
Center for Plasma and Fusion Studies, Korea Advanced Institute of Science and Technology, 373-1 Kusongdong, Yuseongku, Taejon 305-701, Korea

M. S. Chance, J. Manickam, N. Pomphrey, and M. Okabayashi
Princeton Plasma Physics Laboratory, P.O. Box 451, Princeton, New Jersey 08543

(Received 21 August 1997; accepted 8 December 1997)

The results of two-dimensional calculations of eddy currents induced on external conducting walls surrounding a tokamak are reported. The computed eddy currents are generated by low-*n* ($n=1,2,3$) external ideal-magnetohydrodynamic (MHD) instabilities. For a given toroidal mode number n the eddy current patterns are found to be very similar in a variety of plasma configurations, e.g., different edge safety factors and different plasma–wall separation distances, in high beta plasmas. This result is promising for the design of active feedback coils for the stabilization of the resistive wall mode. Also, the effects of having a partial wall that has a poloidal gap on the outboard side are considered. Using the expected gap size in the proposed Korea Superconducting Tokamak Advanced Research (KSTAR) [''The KSTAR tokmak,'' in *Proceedings of the 17th Symposium on Fusion Engineering*, San Diego, 1997 (Institute of Electrical and Electronics Engineers, New York, in press), Paper No. O3.1], the calculation shows that active coils mounted behind the partial walls (the KSTAR passive plates) cover an adequate portion of the eddy current dominant region, enabling feedback stabilization. © *1998 American Institute of Physics.* [S1070-664X(98)03203-0]

I. INTRODUCTION

The ideal external kink mode is widely considered to be one of the plasma-beta-limiting instabilities in present day tokamaks, and represents a major limiting factor for advanced regimes such as the reversed shear mode.[1] The instability is easily stabilized if an ideal perfectly conducting wall is placed close enough to the plasma.[2] However, since the actual wall is resistive, the ideal external kink mode is not completely stabilized and instead transforms into the resistive wall mode (RWM).[3,4] Then the instability would grow on an L/R time scale with the helical flux loss through the wall, fairly slow compared to the typical fast magnetohydrodynamic (MHD) time scale. This is still a major concern, especially for long-pulse high-beta operations in future advanced machines such as the proposed Korea Superconducting Tokamak Advanced Research (KSTAR)[5] and the International Thermonuclear Experimental Reactor (ITER).[6] Several schemes for the stabilization of the mode have been proposed, e.g., stabilization by a strong toroidal rotation of plasma with the inclusion of a damping mechanism.[7] Another way to stabilize this mode, which may be more reactor relevant, is to install a system of active feedback coils in association with the external wall.[8,9] The function of the feedback system is to compensate for the helical flux loss in a two-dimensional manner, and to sustain the ideal MHD (with ideal wall) external mode-induced flux pattern as closely as possible until the mode is stabilized. Therefore, for the successful implementation of such a system, it is essential to study the two-dimensional patterns of eddy currents induced on the external conducting wall.[10] In this work, we have done such calculations using the PEST-VACUUM code.[10,11] The calculations involve the ideal-MHD low-*n* ($n=1,2,3$) external modes. Also, the calculations cover various physical situations such as different safety factor q profiles, different plasma–wall separation distances, conducting walls with and without an outboard side gap, and different plasma shapes. From the viewpoint of utilizing this method, there are two major issues that we wish to consider in this paper: (i) Is it possible to design a robust system of active feedback coils that would be effective in a variety of plasma configurations?; and (ii) what is the effect of a poloidal gap in a partial wall?

The paper is organized as follows. In Sec. II, the physical interpretations on the computed eddy current are presented. Then, in Sec. III, we discuss the effects of incomplete, partial walls with an outboard (toroidally continuous) poloidal gap. Some relevant discussions and summary are presented in Sec. IV.

II. PHYSICAL INTERPRETATION OF EDDY CURRENT PATTERNS

In this section, we wish to demonstrate that the induced eddy current patterns in *high β, D-shaped, finite aspect ratio* plasmas are similar in various physical conditions such as different edge q values and wall distances. This is important since it promises a simple design for the feedback coil system that will be effective over a wide range of discharges.

a)Electronic mail: dylee@yebbi.kaist.ac.kr

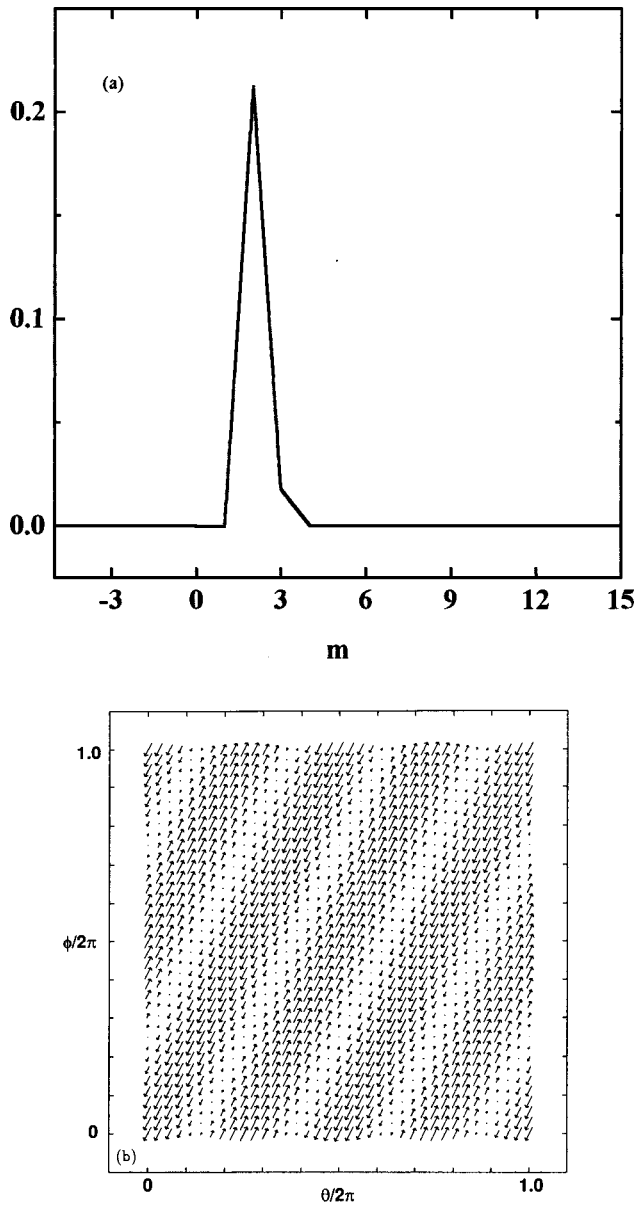

FIG. 1. (a) A plot of $(m-nq)\xi_m$, which is proportional to the normal component of the perturbed magnetic field on the plasma surface, for different poloidal harmonic number m. A circular shape plasma is considered, in which $q_{\text{edge}}=1.9$, $R/a=100$, and $\beta=0.001\%$. (b) Display of eddy currents in the θ-ϕ plane of the conformal wall. The eddy current is induced by an $n=1$ external instability.

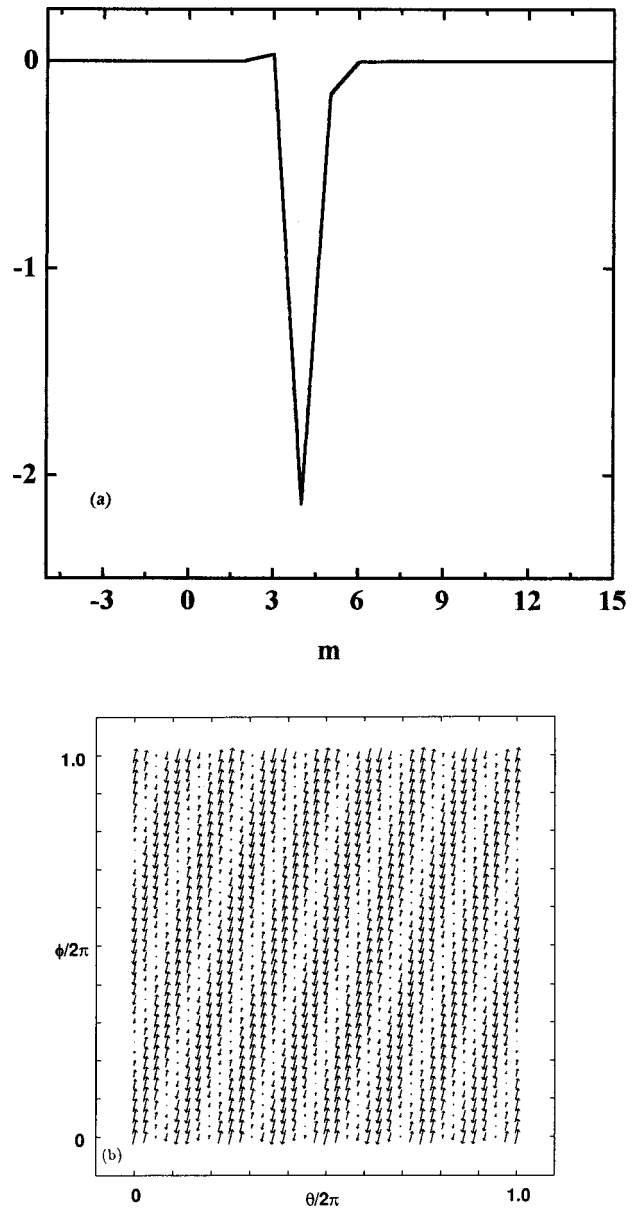

FIG. 2. (a) The same plot as in Fig. 1(a), but for a different circular plasma, where $q_{\text{edge}}=3.78$, $R/a=100$, and $\beta=0.001\%$. (b) The same plot as in Fig. 1(b).

We consider the situation where the plasma is completely surrounded by a conformal wall, i.e. a wall with the same shape as the plasma at a uniform distance, b. The wall in the PEST-VACUUM code is taken to be perfectly conducting. The eddy currents in such an ideal wall are induced by low-n, $n=1,2,3$, ideal-MHD external kink instabilities. (This eddy current will, of course, decay away on an L/R time scale in the actual *resistive* wall, leading to the RWM. A smart system consisting of the active feedback coils plus the resistive walls that can sustain the eddy current pattern should stabilize the RWM.) Calculations include different plasma shapes as well as different aspect ratio, R/a, plasmas. Given a particular shape of plasma and a toroidal mode number, n, calculations are performed for equilibria with different q profiles. We also consider various distances between the plasma and the stabilizing wall.

A. Circular, nearly zero β, very large aspect ratio case

We first consider a plasma of a circular cross section with a very large aspect ratio, $R/a=100$. The plasma beta is nearly zero, $\beta=0.001\%$. (Hereafter, β is given in %.) This plasma mimics the conventional cylindrical limit, and we can study purely current-driven kink modes. We present two cases with different q_{edge} values. Calculations are done for the $n=1$ external kink instability.

In the first case $q_{\text{edge}}=1.93$, and an external wall is placed at $b=0.3a$ from the plasma surface. Figure 1(a) plots $(m-nq)\xi_m$, which is proportional to the normal component

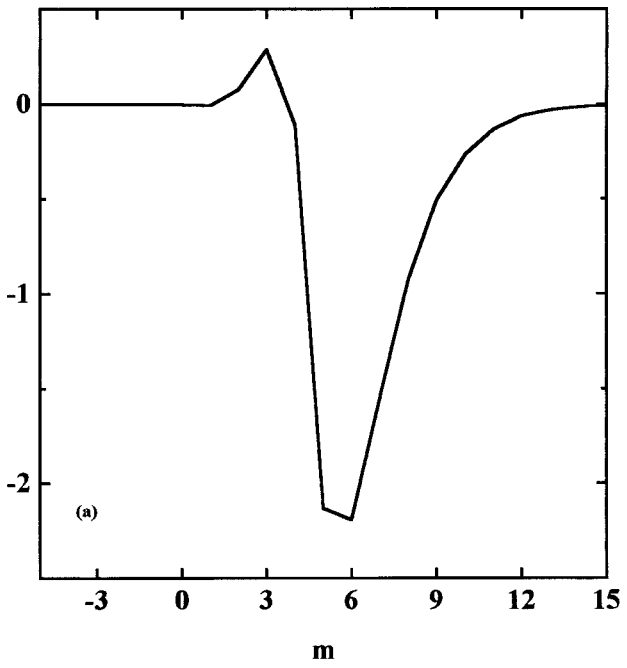

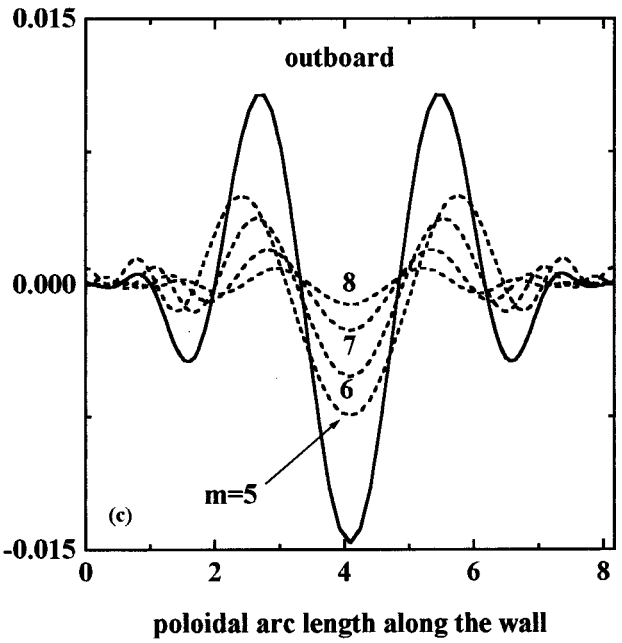

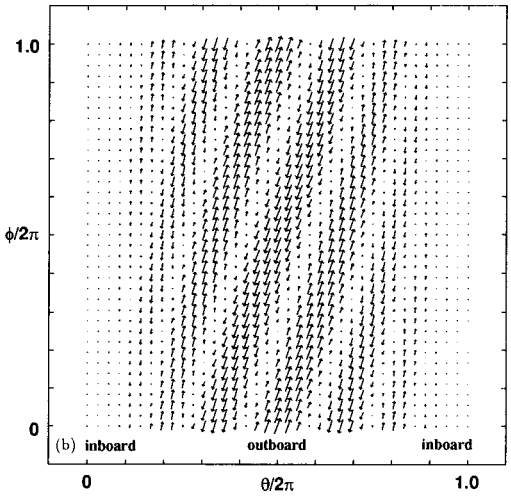

FIG. 3. (a) The same plot as in Fig. 1(a), but for the circular plasma, where $q_{\text{edge}}=3.95$, $R/a=100$, and $\beta=0.08\%$. (b) The same plot as in Fig. 1(b). (c) A plot of the perturbed vacuum scalar potential along the poloidal direction in the wall, χ_m, for several major m components, $m=5-8$ (dotted lines), and the total χ (solid line). Only the real part is plotted.

of the perturbed magnetic field on the plasma surface. As expected, the $m=2$ contribution is absolutely dominant on the plasma surface. Shown in Fig. 1(b) is the induced eddy current pattern on the wall. It clearly shows the $m=2$ poloidal harmonic structure.

Similar calculations are done for a different equilibrium where $q_{\text{edge}}=3.78$. The wall is placed at the same distance, $b=0.3a$. With the change in q_{edge} the dominant m is now 4. As before, Fig. 2(a) shows the perturbed magnetic field on the plasma surface, and Fig. 2(b) shows the corresponding eddy pattern on the wall. Again, we note that the wall response is consistent with the plasma surface perturbation as $m=4$ is the only dominant harmonic in both the plasma surface and the wall.

It is clear that the eddy response in the wall is determined by q_{edge} values, and is consistent with the plasma surface motion, in the nearly zero β, very large aspect ratio, circular plasma. This is, in fact, consistent with what may be obtained from an analytical calculation using the conventional low β large aspect ratio cylindrical limit.

B. Finite β effect

We next consider the effect of finite β. As before the plasma shape is circular, and the aspect ratio is 100. The plasma β is, however, increased by a factor of nearly 100, i.e., $\beta=0.08$, and $q_{\text{edge}}=3.95$. The $n=1$ external kink with the wall distance of $0.3a$ is considered.

Figure 3(a) shows the perturbed magnetic field on the plasma surface in which $m=5$ and 6 are now major contributors. Figure 3(b) displays the induced eddy current pattern on the wall. In contrast to the result of Fig. 2 of the previous section, the pattern around the inboard midplane has nearly disappeared. Also, inside the eddy current dominant region, it appears to have the poloidal structure with lower periodicity than what one would expect from the surface perturbation [Fig. 3(a)]. This is due to the finite β ballooning-like effect. Figure 3(c) displays the scalar poten-

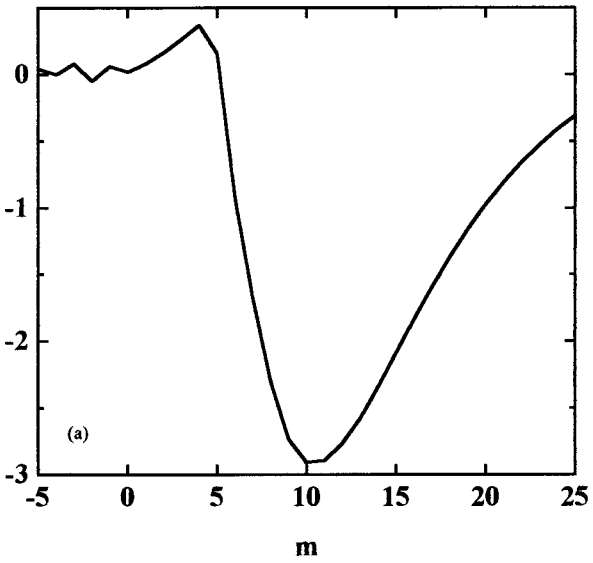

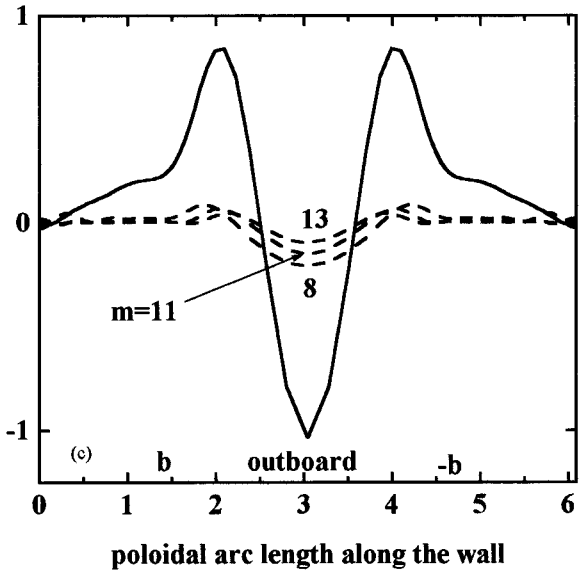

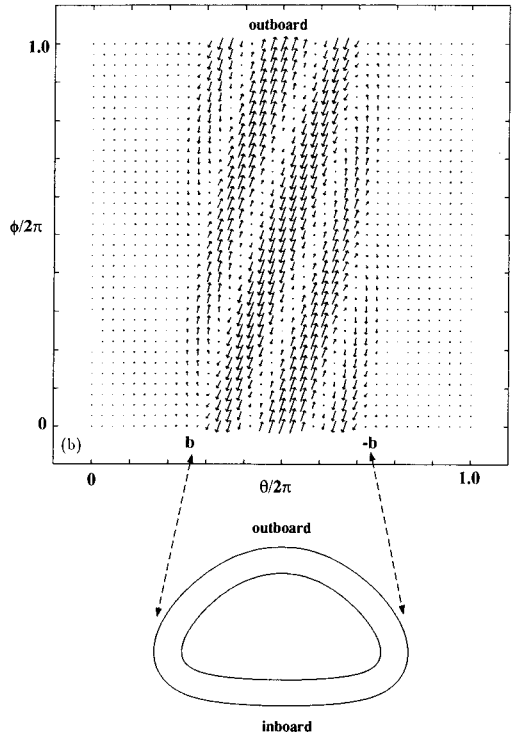

FIG. 4. (a) A plot of $(m-nq)\xi_m$ on the surface of the D shaped plasma, where $q_{\text{edge}}=5.5$, $R/a=3.6$, β=4.3%, and $\beta_n=4.5$. (b) A display of the eddy current. Also sketched is the plasma surrounded by the conformal wall. The eddy dominant region is marked to be from b to $-b$, as indicated by the arrows. (c) A plot of χ_m for several major m components (dotted lines) and the total χ (solid line) along the poloidal direction on the wall.

tial response on the wall, χ_m, for several major-contributing m components, $m=5-8$, as well as the total χ. Here the magnetic field in the vacuum $\mathbf{B}_v=\nabla\chi$, and the induced eddy current on the wall are computed by $\mathbf{K}=\mathbf{n}\times\nabla\chi_{\text{wall}}$.[10] The χ is the sum over contributions from all m components. The amplitudes of each m component all decay away from the outboard midplane along the poloidal direction. This wipes out the contributions in the inboard region, and the net result is that the total χ is left with seemingly lower harmonic structure within the eddy dominant region. This kind of effect is easily expected to be more significant in much higher β deformed plasmas, as discussed in Sect. II D.

C. Finite aspect ratio effect

We have also considered cases where the aspect ratio of the circular plasma is as low as 3.6. In order to see the effect purely from the aspect ratio, however, the plasma β is kept to be nearly zero. The computed eddy current due to $n=1$ external instability has showed some ballooning-like effect due to the reduced aspect ratio. The effect, however, has appeared to be much less significant than that of finite β.

D. D-shaped, high β tokamak plasma

Now we turn to the realistic case where there exist simultaneously both effects due to the finite β and aspect ratio. In the computaion results presented below, the plasma is D shaped with an elongation of 1.8 and triangularity of 0.5 at the 95% flux surface, and has an aspect ratio of 3.6 with a major radius, $R=1.8$ m, and a minor radius, $a=0.5$ m. This plasma is, in fact, consistent with the proposed KSTAR plasma.[5] We have computed eddy currents in various situa-

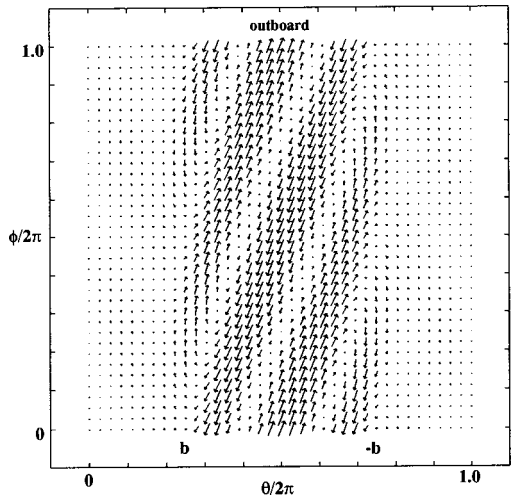

FIG. 5. A similar display of the eddy current for the D-shaped plasma, but where $q_{\text{edge}}=3.86$, $R/a=3.6$, $\beta=7.8\%$, and $\beta_n=6$. The eddy dominant region is marked to be from b to $-b$.

tions in very high β regimes. In particular, these include various safety factor profiles $q(\psi)$ and plasma–wall separation distances. We have found that for a given n number, all patterns of the calculated eddy current have remarkably the same structure. The interpretation similar to that in Sec. II B is given as follows.

Figure 4(a) shows $(m-nq)\xi_m$ against m on the surface of a plasma in which $q_{\text{edge}}=5.5$ and $\beta=4.3$ ($\beta_n=4.5$). An $n=1$ mode is considered. The plot reflects the contributions from various m components, $m=10$ or so being the dominant. As shown in Fig. 4(b), the corresponding eddy current is induced mostly around the outboard side due to the strong ballooning nature in the deformed high beta equilibrium. The eddy dominant region in the external wall is marked to be from b to $-b$ in the figure, and the wall is placed at $b/a=0.5$. This ballooning nature is clearly seen in Fig. 4(c), which plots χ_m for several major m components as well as the total χ along the poloidal direction on the wall. As in Sec. II B, all m components on the wall largely decay away from the outboard midplane along the poloidal direction. This results in the periodic behavior of the total χ with an effective poloidal wave number $m_{\text{eff}}\simeq 1.5$ *inside the eddy dominant region* b to $-b$. This is found to be always the case in all of our calculations for different q profiles, different plasma–wall separation distances, etc. The eddy current shown in Fig. 5 is another example induced by an $n=1$ mode in a different plasma in which $q_{\text{edge}}=3.86$ and $\beta=7.8$ ($\beta_n=6$). This calculation uses the same wall distance, $b/a=0.5$. (The choice of this particular wall distance is somewhat arbitrary, but the eddy patterns for different wall distances, in fact, remain nearly the same.) The eddy pattern in Fig. 5 is nearly identical to that of Fig. 4(b) in their helicities as well as in the poloidal extent.

What we call here the *ballooning effect* is therefore responsible for all eddy current patterns being so similar in various situations in high β deformed plasmas.

We have also done similar calculations for $n=2$ and 3 modes. In some cases, these modes can be more unstable

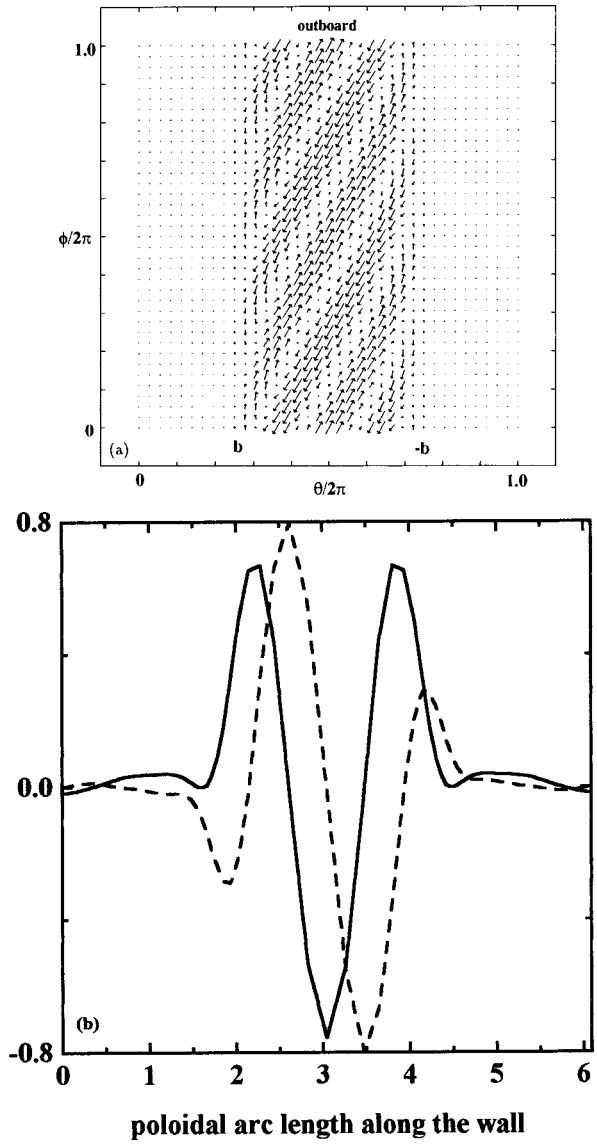

FIG. 6. (a) A plot of the eddy current induced by an $n=2$ mode for the plasma of Fig. 5. (b) A plot of the real and imaginary parts of χ for the $n=2$ case along the poloidal direction on the wall.

than the $n=1$ mode. We present two examples in Fig. 6 and Fig. 7 that correspond to $n=2$ and 3 cases, respectively. Computations are done for the same equilibrium as in Fig. 5 using the same wall distance of $0.5a$. Again, the patterns have well-defined helicities. In addition, a higher-n mode has a slightly smaller poloidal extent in the current coverage than that of the lower-n mode. Figures 6(b) and 7(b) show the scalar potential χ on the wall for [Fig. 6(b)] the $n=2$ case and [Fig. 7(b)] the $n=3$ case, respectively. We notice that the ballooning effect in the $n=2$ and $n=3$ cases is even stronger than the $n=1$ case.

III. EFFECT OF PARTIAL WALL

In the previous section, we have observed the remarkably systematic structure in eddy current responses. This is due to the strong ballooning nature on the outboard side in high β plasmas. On the other hand, the external conducting walls in present day devices, both vacuum vessel and passive

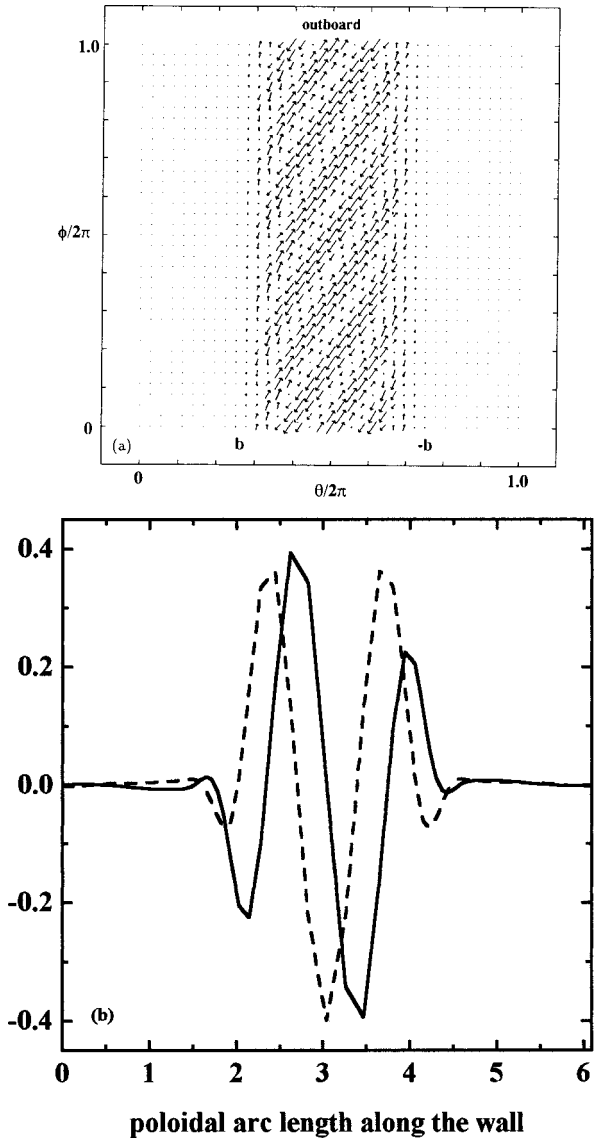

FIG. 7. (a) A plot of the eddy current induced by an $n=3$ mode for the plasma of Fig. 5. (b) A plot of the real and imaginary parts of χ for the $n=3$ case along the poloidal direction on the wall.

plates, necessarily allow some vacuum gap for the access of neutral beam ports and other diagnostics near the outboard midplane, where the same ballooning effect is most significant. The amount of the external conducting material on the outboard side is crucial in achieving high β plasma by the feedback control of the external mode. The sufficient amount of the passive wall should be located close enough to the plasma so that the ideal external kink mode can first transform itself into the RWM branch. This is particularly true and important for the reverse shear mode.[2] Then a successful feedback system of active coils, for example, will stabilize the RWM, enabling the access to the high β kink-stable plasma. Therefore, a study of the outboard gap effect is essential. We have studied such effects using the PEST-VACUUM code for the KSTAR plasmas. The partial wall used in the simulation has a toroidally continuous poloidal gap on the outboard side. We have considered the various gap sizes and plasma–wall separation distances.

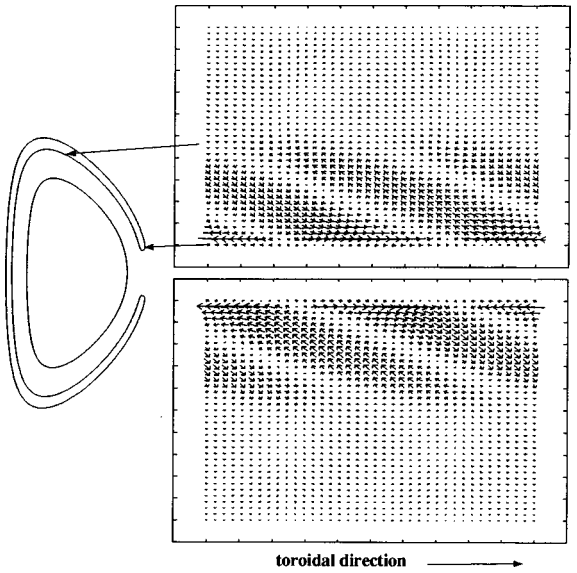

FIG. 8. A display of the eddy current induced on the partial wall by an $n=1$ mode for the plasma of Fig. 5. The eddy dominant region along the poloidal direction is indicated by the arrows.

Figure 8 shows the eddy current on a partial wall induced by an $n=1$ mode instability in a KSTAR plasma with $q_{\text{edge}}=3.86$. The outboard gap size in this partial wall is relatively small. Consequently, the wall covers the most poloidal portion of the outboard region as much as a complete conformal wall would do. However, this gap size may not be realistic for the access of the neutral beam port and other diagnostics.

To be realistic, we now double the size of the gap. In fact, this gap size is roughly consistent with that of the passive plates in the proposed KSTAR tokamak. Figure 9 displays the eddy current induced by the $n=1$ mode on such a partial wall. The eddy current dominant region is now more

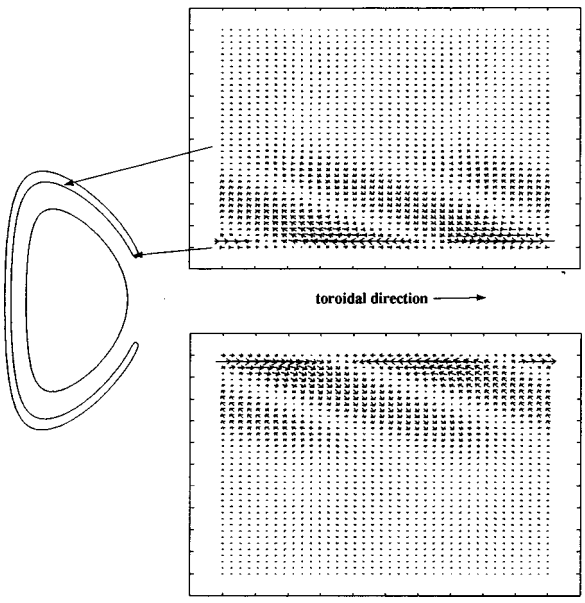

FIG. 9. The same display as in Fig. 9, but the gap size in the partial wall has been doubled.

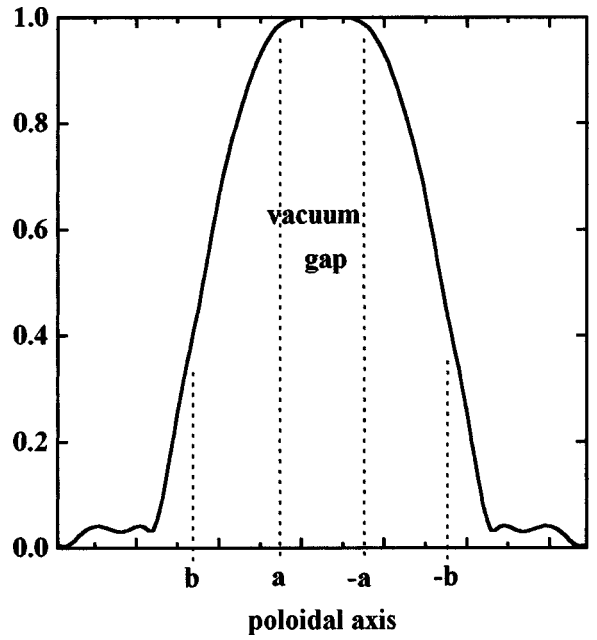

FIG. 10. A plot of the normal component amplitude of the perturbed magnetic field that would arise if there were placed no external wall. The calculation is done for the $n=1$ mode of Fig. 9, and plotted along the poloidal direction on a virtual fake wall at $0.3a$.

limited, as indicated by the arrows in the figure. However, the expected design of the KSTAR[5] is that the passive plates will sufficiently cover the same eddy dominant region. Another way to look at the wall coverage matter is given in Fig. 10. Plotted in the figure is the normal component amplitude of the perturbed vacuum field that would arise due to the $n=1$ plasma motion if there were placed no external wall. The plot represents the calculation along the poloidal direction on *a virtual fake* wall. An ideal *complete conformal* wall, if placed at the same position as the virtual wall, would generate the eddy current to exactly cancel out the normal magnetic field predicted in Fig. 10. The *partial wall* of Fig. 9 or the KSTAR passive plates (assuming the perfect conductivity) covering the region, $a(-a)$ to $b(-b)$, will function in the same way, except in the vacuum gap region, where no eddy current flows.

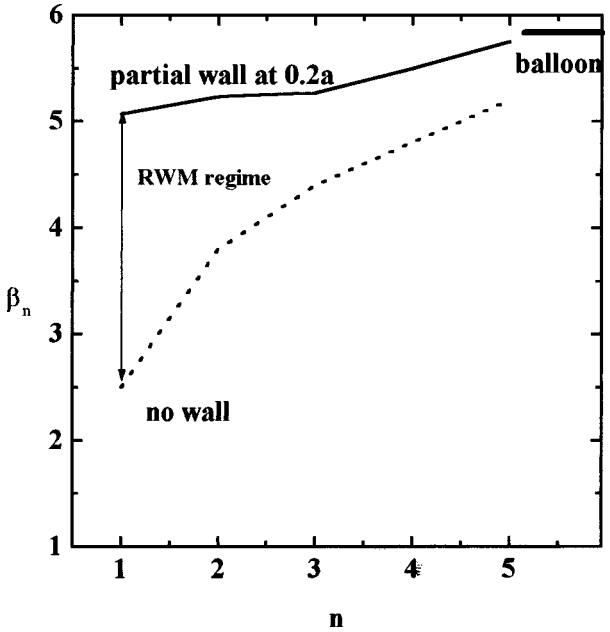

FIG. 11. A plot of β_n limits for the toroidal number n of 1–5 in the KSTAR reversed shear mode. The gap size used for the partial wall (placed at $0.2a$) is consistent with that of the KSTAR passive plates. The stability limits for the no wall case as well as for the high-n ballooning are indicated as ''no wall'' and ''balloon,'' respectively.

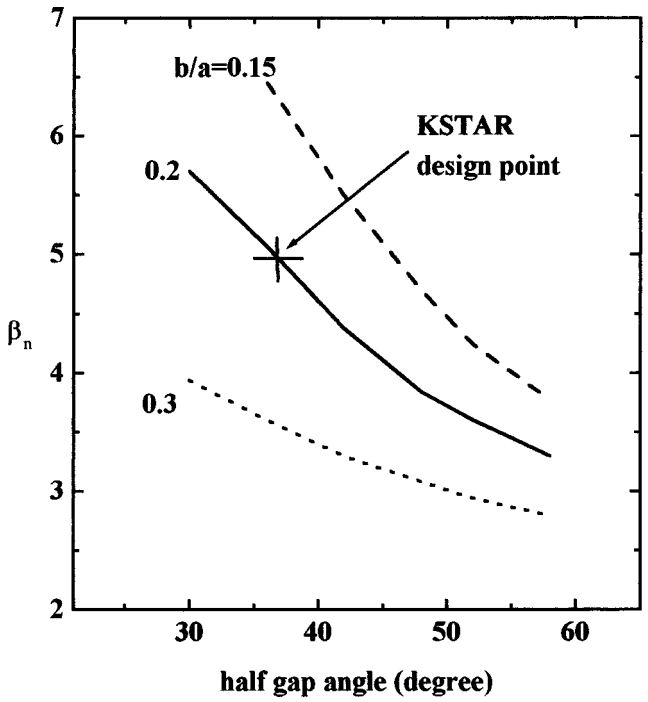

FIG. 12. A plot of the β_n limits for the $n=1$ mode in the KSTAR reverse shear equilibria over a range of the vacuum gap size at three different plasma–wall separation distances. The half-gap angle is in units of degrees and is defined to increase away from the outboard midplane along the poloidal direction.

In order to see the effectiveness of the partial wall in stabilizing the high β external kink, we have done an extensive stability analysis in the KSTAR plasma. The analysis has taken into account the profile optimizations of pressure and current density along with the bootstrap current alignment requirement.[2] The KSTAR passive plates have been simulated using the partial wall shape of Fig. 9 and again assumed to be perfectly conducting. Stability to the $n=1-5$ modes as well as the high-n ballooning has been tested. Figure 11 summarizes the results for the reverse shear equilibria. Without the external wall, the β limit is $\beta_n=2.5$ set by the $n=1$ ideal kink mode. Placing the partial wall at $0.2a$, which is roughly the present design point, we find the substantial improvement in β limit that the ideal low-n modes can be stabilized at a β_n value of up to 5 in the reverse shear equilibria. The region between $\beta_n=2.5$ (no wall) and $\beta_n=5$ (ideal partial wall) corresponds to the RWM regime. Therefore, the predicted β limits with the ideal wall can only be achieved if the RWM is stabilized by the feedback control. We have also calculated the effects of varying the gap size as well as the plasma–wall separation distance.

Figure 12 shows the results for the $n=1$ mode in the reverse shear equilibria. It shows the obvious trend that the β limit decreases as the gap size and/or the separation distance increases. It appears that both the plasma–wall separation distance and the gap size are equally important. In both regards, the wall coverage by the KSTAR passive plates is adequate enough to stabilize the ideal-MHD high-β external modes, transforming the modes into the RWM branch. It seems adequate to utilize the feedback coils behind such passive plates to further stabilize the RWM.

IV. SUMMARY AND CONCLUSIONS

The RWM grows as a modified ideal kink due to the finite resistivity of the external walls. In order to study the feasibility of implementing an integrated feedback system (resistive walls plus active coils) for the RWM control, we have considered the following two major issues. First, the major function of the active coils is to make the integrated feedback system act like an ideal wall. Then, such an integrated system should be able to sustain the eddy current pattern as closely as possible that an ideal external kink mode would generate on an ideal wall, until the mode is stabilized. Theoretical examination of such eddy currents in ideal walls is useful, and thus will guide the design of the active coil system for the RWM control. In this paper, we have reported the PEST-VACUUM code result of the eddy current on external conducting walls induced by low-n external ideal MHD instabilities. We have found an important new result that, for a given toroidal mode number n, all the calculated eddy current patterns in high β deformed plasmas are remarkably similar in various physical conditions, including different safety factor profiles and plasma–wall separation distances. This is due to the strong ballooning effect in high β deformed plasmas, which wipes out the wall responses away from the outboard midplane along the poloidal direction. This observation makes it possible to design the feedback coil system in a robust, not too complicated, way for the RWM stabilization: A fixed set of coils can cover various conditions such as various q_{edge} discharges, etc.

Second, a prerequisite to achieve the high β external kink-stable plasma by the feedback control with the integrated feedback system is that the ideal high β external kink first needs to be slowed down to a sufficiently longer time scale. This requires the sufficient amount of the passive material with the sufficient proximity to the plasma surface, particulary on the outboard side. For the realistic partial wall that has a vacuum, toroidally continuous, poloidal gap on the outboard side, it is thus important to ensure that the size of the gap is not too large. Our calculations have included a practical and realistic case by taking the relevant parameters from the proposed KSTAR tokamak. It appears that the partial walls, the closely fitted passive plates in the KSTAR, stabilize the low-n ideal modes in very high β equilibria: β_n of up to 5 is found to be stable in the reverse shear equilibrium, assuming the wall is ideal. Indeed, the KSTAR passive plates cover the sufficient portion of the eddy dominant domain. The predicted β limits can only be achieved if the RWM is stabilized, of course. The external windings of the feedback coils behind such external walls will be very feasible for the RWM control.

ACKNOWLEDGMENTS

One of the authors (D.Y.L) is indebted to Princeton Plasma Physics Laboratory Theory Division for the hospitality during his visit. He is also grateful to H. G. Jhang and the KSTAR team for helpful discussions.

This work was supported by the Korea Ministry of Science and Technology under the Korea Superconducting Tokamak Advanced Research project.

[1] C. Kessel, J. Manickam, G. Rewoldt, and W. Tang, Phys. Rev. Lett. **72**, 1212 (1994).
[2] J. Manickam, M. S. Chance, S. C. Jardin, C. Kessel, D. Monticello, N. Pomphrey, A. Reiman, C. Wang, and L. E. Zakharov, Phys. Plasmas **1**, 1601 (1994).
[3] C. G. Gimblett, Nucl. Fusion **36**, 617 (1986).
[4] J. P. Freidberg, *Ideal Magnetohydrodynamics* (Plenum, New York, 1987), pp. 307–315.
[5] D. I. Choi, G. S. Lee, Jinchoon Kim, H. K. Park, C. S. Chang, B. H. Choi, K. Kim, M. H. Choi, G. H. Neilson, S. Baang, S. Bernabei, T. Brown, H. Y. Chang, C. H. Cho, S. Cho, Y. S. Cho, K. H. Chung, Kie-Hyung Chung, F. Dahlgren, L. Grisham, J. H. Han, N. I. Huh, S. M. Hwang, Y. S. Hwang, D. Hill, B. G. Hong, S. H. Hong, K. H. Im, S. R. In, S. Jardin, H. G. Jhang, M. Joo, Y. S. Jung, C. Kessel, D. L. Kim, H. S. Kim, J. Y. Kim, Y. J. Kim, W. C. Kim, M. C. Kyum, D. Y. Lee, B. J. Lee, D. K. Lee, S. G. Lee, J. Y. Lim, J. Manickam, B. Montgomery, W. Namkung, W. Nevins, Y. K. Oh, J. H. Park, N. Pomphrey, W. Reiersen, J. H. Schultz, J. A. Schmidt, R. T. Simmons, J. C. Sinnis, D. W. Swain, L. Sevier, P. W. Wang, J. G. Yang, G. H. You, B. J. Yoon, and K. M. Young, ''The KSTAR tokamak,'' in *Proceedings of the 17th Symposium on Fusion Engineering,* San Diego, 1997 (Institute of Electrical and Electronics Engineers, New York, in press), Paper No. O3.1.
[6] J. C. Wesley and the ITER Joint Central Team , Phys. Plasmas **4**, 2642 (1997).
[7] A. Bonderson and D. J. Ward, Phys. Rev. Lett. **72**, 2709 (1994).
[8] C. M. Bishop, Plasma Phys. Controlled Fusion **31**, 1179 (1989).
[9] R. Fitzpatrick and T. H. Jensen, Phys. Plasmas **3**, 2641 (1996).
[10] M. S. Chance, Phys. Plasmas **4**, 2161 (1997).
[11] R. G. Grimm, J. M. Greene, and J. L. Johnson, in *Methods in Computational Physics*, edited by J. Killeen (Academic Press, New York, 1976), Vol. 16 of *Controlled Fusion,* pp. 253–280.